are smaller, for the same reasons discussed in reference to steel structural plate.

CONCLUSION

The SCI design procedure provides a rational method for determination of both minimum depths of cover and maximum fill heights. Values of minimum cover calculated using the SCI method compare well with design experience as reflected in values from published fill-height tables. The advantage of the SCI method is that it provides a rational procedure for including the effects of all the variables that affect minimum cover, namely diameter, corrugation size, metal thickness, yield stress, backfill type, degree of compaction, and magnitude of live load. The ability to account for the effects of these factors in a rational way is especially important for long-span culverts, where cover depths are often small.

Values of maximum cover calculated using the SCI method are somewhat smaller than those calculated using the AISI and NCSPA procedure. They are considerably larger than those calculated using the DOT, FHWA, and BPR procedure, especially in cases where the latter values are determined by consideration of calculated deflections.

Although all the examples of the use of the SCI method in this paper are for circular pipes, the method is also applicable to pipe-arch and arch structures. It is particularly useful for design of long-span culvert structures, for which considerations of performance under live load with shallow cover are of prime importance.

ACKNOWLEDGMENT

I am grateful to Kaiser Aluminum and Chemical Sales, Inc., for sponsoring the research studies that led to the development of the SCI method, and to Kai Wong and Gary Jaworski of the University of California, Berkeley, geotechnical research staff, who performed the finite element analyses.

REFERENCES

1. J. M. Duncan. Behavior and Design of Long-Span Metal Culvert Structures. Paper presented at the Technical Session on Soil-Structure Interaction for Shallow Foundations and Buried Structures, ASCE National Convention, San Francisco, Oct. 1977.
2. J. R. Allgood and S. K. Takahashi. Balanced Design and Finite Element Analysis of Culverts. HRB, Highway Research Record 413, 1972, pp. 45-56.
3. J. R. Abel, R. Mark, and R. Richards. Stresses Around Flexible Elliptic Pipes. Journal of the Soil Mechanics and Foundations Division, Proc., ASCE, Vol. 99, No. SM7, 1973, pp. 509-526.
4. M. G. Katona, J. B. Forrest, R. J. Odello, and J. R. Allgood. Computer Design and Analysis of Pipe Culvert. U.S. Naval Civil Engineering Laboratory, Port Hueneme, Internal Technical Rept., CA 51-040, FHWA 3-1-1170, 1974.
5. K. S. Wong and J. M. Duncan. Hyperbolic Stress-Strain Parameters for Nonlinear Analyses of Stresses and Movements in Earth Masses. University of California, Berkeley, Geotechnical Engineering Rept., TE 74-3, 1974.
6. E. W. Wolf and M. Townsend. Corrugated Metal Pipe: Structural Design Criteria and Recommended Installation Practice. U.S. Bureau of Public Roads, U.S. Government Printing Office, 1970.
7. Handbook of Steel Drainage and Highway Construction Products, 2nd Ed. American Iron and Steel Institute, New York, 1971.
8. Corrugated Steel Pipe. National Corrugated Steel Pipe Association, Chicago.
9. Aluminum Storm Sewers. Kaiser Aluminum and Chemical Sales, Inc., Oakland, CA, 1976.
10. Fill Heights for 3- by 1-in. Corrugated Steel Pipe in 'Good' Backfill. United States Steel Corp., Pittsburgh, 1967.

Publication of this paper sponsored by Committee on Subsurface Soil-Structure Interaction.

Analysis of Long-Span Culverts by the Finite Element Method

Michael G. Katona, University of Notre Dame, Notre Dame, Indiana

The long-span culvert is a synergistic unit composed of a corrugated metal liner and a compacted soil envelope that surrounds the liner. Conceptually, the system is very simple and, therefore, economically attractive as a bridge substitute. Analytically, however, the system is not simple because of the modeling difficulties associated with soil-structure interaction. Using the finite element method, this study investigates the influence of fundamental modeling assumptions on the behavior of long-span culverts. Two basic modeling assumptions are examined: large deformation theory versus small deformation theory and monolith structure versus incremented structure. In addition, the sensitivity of the following parameters are determined: compaction loads, soil stiffness, liner gage, liner shape, and special features of manufacturers. Results are shown graphically by comparing crown displacement histories between parametric families. Comparisons of maximum moment and thrust are also reported. Based on these studies, recommendations for analytical modeling techniques are summarized. The intent of this study is to provide a foundation for other studies. A systematic investigation of modeling assumptions and parameter sensitivity is a necessary step toward an analytical model for long-span culverts.

The long span is an arch or closed-shaped corrugated metal liner surrounded by compacted soil, where the horizontal span measures from 5 to 15 m (15 to 50 ft) or more. A primary use is to serve as a bridge substitute. To date, more than 600 long-span systems have been installed, and manufacturers estimate a cost savings from 30 to 75 percent over comparable conventional bridge structures. In view of the current bridge repair and replacement problem in the United States

(the Federal Highway Administration estimates that nearly 18 percent of all U.S. bridges are in disrepair or functionally obsolete), use of long-span structures will probably increase markedly. Accordingly, analytical studies of long spans are timely and can lead to improved design methods. However, in order to properly analyze long-span systems, the basic construction process must be understood.

The long span is usually constructed by bolting together curved, structural plates of corrugated metal into the shape of an arch, with the ends anchored into concrete footings. Or in some cases, elliptical or inverted pear-shaped sections are used with special beddings instead of footings. Figure 1 illustrates some basic shapes and nomenclature popularly used for long-span structures. The most important step in the construction process is placing soil (backfilling) around the corrugated metal liner. The soil must be of good structural quality and properly compacted one lift at a time, symmetrically on both sides of the liner. During this process, the lateral soil pressure moves the sides of the liner inward and the crown upward (peaking).

Figure 1. Typical long-span liner shapes and nomenclature.

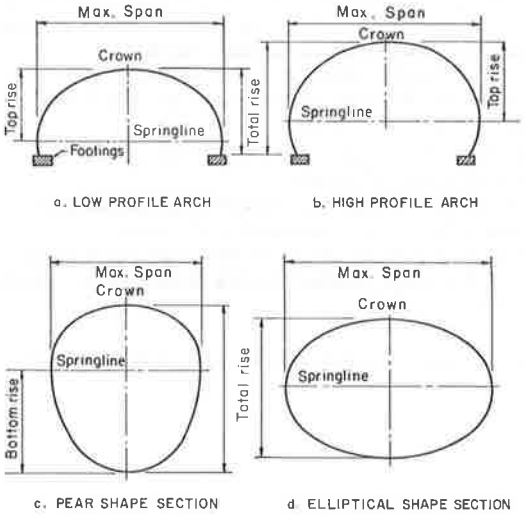

Figure 2. Special features of long spans.

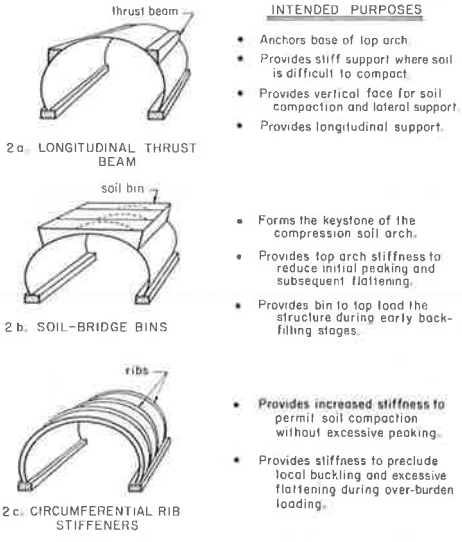

Once the backfill soil is level with the crown, subsequent soil lifts reverse this trend by pushing the crown downward and the sides outward. Outward movement mobilizes lateral soil resistance, which limits both lateral and vertical movement.

Indeed, the interaction of the soil and liner working in tandem provides the remarkable structural integrity of the long-span system. Either component, liner or soil, acting by itself would be wholly inadequate to support the loads. To promote and improve this synergistic relationship between liner and soil, several special features have been employed by various manufacturers. Some commonly used features are thrust beam, soil bin, and rib stiffeners (shown in Figure 2). Additional background information can be found in the excellent survey by Selig and others (1).

ANALYSIS-DESIGN PROBLEM

For the most part, current design methods are based on experience rather than on a viable analytical model (1). This is because a reasonable analytical model is complicated even though the long span is a conceptually simple system. Complications are due to the soil-structure interaction phenomena; that is, a long-span model must include the soil as a structural element—it cannot simply assume the soil loads on the liner. Other modeling difficulties include incremental construction (i.e., modeling the soil placement schedule during construction), various shapes, footings, and special features, as well as consideration of soil compaction, interface slippage, and other nonlinear behavior.

The finite element method (FEM) appears to be the best method for formulating and solving this complicated boundary value problem. Indeed, this is a singular point of common agreement among investigators of soil-structure interaction (1, 2, 3, 4, 5, 6, 7). In particular, recent applications of FEM to long-span systems show great promise for understanding long-span behavior (8, 9, 10). FEM is well established and has become an indispensable tool in structural research (11).

The objective is to present analytical results of a parameter study that compares various modeling assumptions of long-span culverts. The following parameters are examined using FEM:

1. Influence of large deformation theory versus small deformation theory;
2. Influence of manner of loading (i.e., monolith structure versus incremented structure with and without compaction loads);
3. Effect of fill soil stiffness (modulus);
4. Effect of liner stiffness (gage);
5. Effect of liner shape (high profile, low profile, and ellipse); and
6. Effect of special features (thrust beam, soil bin, and rib stiffeners).

The first two studies deal with the question of how to simulate the real-world behavior of long spans. The remaining studies compare the structural behavior of different idealized systems.

These objectives have a twofold purpose: (a) they provide a foundation or benchmark for other studies to compare with and build on, with the ultimate goal of achieving an accepted model; and (b) they illustrate the comparative performance between various long-span concepts.

To satisfy the objectives, a basic idealization of a typical long-span system is assumed. This basic model is used as a common reference for generating 15 different idealizations by selectively changing the system

Table 1. Parameter identification per FEM solution.

Computer[a] Designation	Liner[b] Shape	Special[c] Features	Loading[d] Method	Compaction[e] Pressure (kPa)	Fill Soil[f] Modulus (kPa)	Liner[g] Thickness Gage
A-A	HP	N	MONO	0.0	13 800	5
A-B	HP	N	MONO	0.0	13 800	5
A	HP	N	MONO	0.0	13 800	5
B	HP	N	INC	0.0	13 800	5
C (Basic)	HP	N	INC	34.5	13 800	5
D	HP	N	INC	69.0	13 800	5
E	HP	N	INC	34.5	6 900	5
F	HP	N	INC	34.5	21 600	5
G	HP	N	INC	34.5	nonlinear	5
H	HP	N	INC	34.5	13 800	10
I	HP	N	INC	34.5	13 800	1
J	LP	N	INC	34.5	13 800	5
K	EL	N	INC	34.5	13 800	5
L	HP	TB	INC	34.5	13 800	5
M	HP	SB	INC	34.5	13 800	5
N	HP	RS	INC	34.5	13 800	5

Note: 1 kPa = 0.15 lb/in^2.

[a] Run No. A-A (small deformation) and A-B are ADINA program, all others are CANDE.
[b] Liner shape: HP = high profile, LP = low profile, EL = ellipse.
[c] Special features: N = liner only, TB = thrust beams, SB = soil bins, RS = rib stiffeners.
[d] Loading method: MONO = monolith system, INC = incremented system, density = 18.9 kN/m^3 (120.96 lb/ft^3).
[e] Compaction pressure is applied to side soil lifts and removed on subsequent lift.
[f] Soil modulus is Young's modulus, Poissons ratio = 0.35 always.
[g] Liner is standard structural steel corrugation 15 x 5 cm (6 x 2 in).

parameters. Table 1 lists each idealization and the system parameters: liner shape, special features, loading method, compaction pressure, soil modulus, and liner gage. The basic idealization is designated as run C and is a high-profile arch, no special features, incremented construction with 34-kPa (5-lb/in^2) temporary compaction pressure; soil modulus is 13 800 kPa (2000 lb/in^2) and liner is 5-gage steel.

Solutions of these idealizations are obtained by the finite element program CANDE (12) except for the case of large deformations, which is solved by program ADINA (13). CANDE is a special-purpose program intended for soil-structure interaction studies and ADINA is a multipurpose program oriented to solid mechanics. Fundamental assumptions common to all solutions are plane-strain geometry, linear material properties (except in one case), and time-independence (i.e., no inertia or viscosity). The soil and footing are assumed to behave as a continuum and the metal liner is treated as a thin shell.

By grouping appropriate solutions, the effect of each parameter can be ascertained by inspecting the key responses—crown deflection, maximum thrust, and maximum moment in the liner wall.

PARAMETER INVESTIGATION

The long-span configuration chosen for the basic model is an 11.0-m (36-ft) high-profile arch with a 3.40-m (11-ft 2-in.) rise. Figure 3 portrays the basic idealization showing the in situ soil zone below the footing and the fill soil zone [18.9 kN/m^3 (120 lb/ft^3)] above the footing level. The soil zones, concrete footing, and metal liner are assumed to be bonded at material interfaces, and each zone is homogeneous with the elastic properties noted at the bottom of the figure.

The FEM discretization of the idealization is shown in Figure 4. Because of symmetry, only half of the system is modeled, with a total of 253 elements. Seventeen beam-column elements are connected to form the metal liner; the 17th element is buried in the concrete footing. The concrete footing (4 elements), in situ soil (90 elements), and fill soil (144 elements) are four-node quadrilateral or three-node triangular continuum elements with two degrees of freedom per node. In the CANDE program the continuum elements include high-order nonconforming displacement functions, whereas in the ADINA program they are standard isoparametric elements.

To accommodate the special features, the basic finite element mesh is altered slightly to model the thrust beam and soil bin. With regard to liner shape, only the bottom half of the mesh is changed to achieve a low profile or elliptical shape.

Large Deformation

This study illustrates the order of the error from using small deformation theory in the analysis of long-span systems. By considering the basic long-span model as a monolith, solutions for large and small deformation theories were obtained by means of the ADINA program (Run A-A and A-B, Table 1). The difference between solutions may be observed in Figure 5 by comparing deformed shapes of the metal liner. Deformed shapes are determined by adding (and magnifying) displacements to the corresponding points of the undeformed position after subtracting vertical rigid body movement of the footing.

The important observation is that the large deformation solution is not significantly different than the small deformation solution; the differences at most are 8 percent at the crown. As a general trend, the large deformation responses are slightly higher in magnitude than the small deformation responses.

For the large deformation theory, both Lagrangian and Eulerian coordinate descriptions give essentially identical results even though the same elastic properties are used in both descriptions. Therefore, it may be concluded that large strains do not come into play so that all differences between large and small deformation solutions are attributed to large rotations.

Figure 1 also illustrates a cross-check between the ADINA and CANDE programs (Run A-A and A, Table 1). The two solutions overlay each other with an error of less than 1 percent, thereby providing validation and confidence in the respective algorithms.

Monolith Versus Incremental

In this study a comparison is made between idealizing the long-span system as monolith versus an incremental system (Run A and B, Table 1). A monolith system may be imagined by assembling the long-span system

Figure 3. Description of basic model idealization.

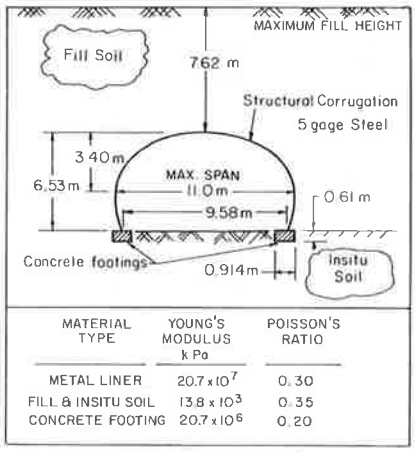

MATERIAL TYPE	YOUNG'S MODULUS k Pa	POISSON'S RATIO
METAL LINER	20.7×10^7	0.30
FILL & INSITU SOIL	13.8×10^3	0.35
CONCRETE FOOTING	20.7×10^6	0.20

Note: 1 m = 3.3 ft, 1 kPa = 0.15 lb/in^2.

Figure 4. FEM representation of basic model.

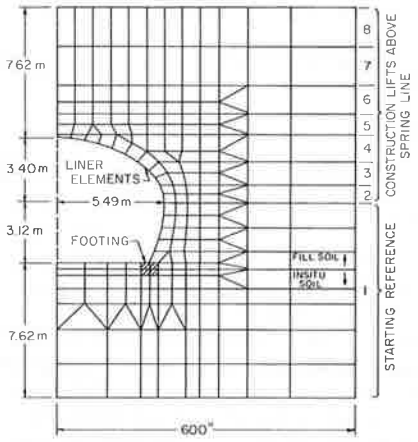

Note: 1 m = 3.3 ft.

Figure 5. Deformed shapes for small and large deformation theories.

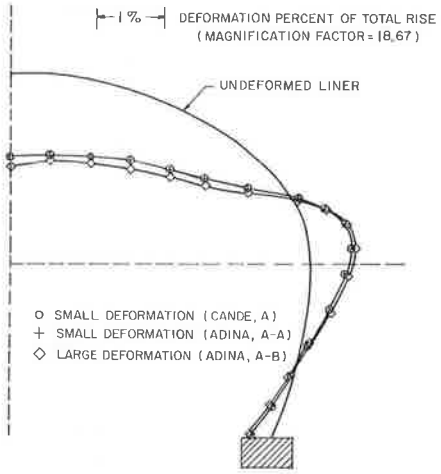

Figure 6. Influence of loading conditions on crown deflection.

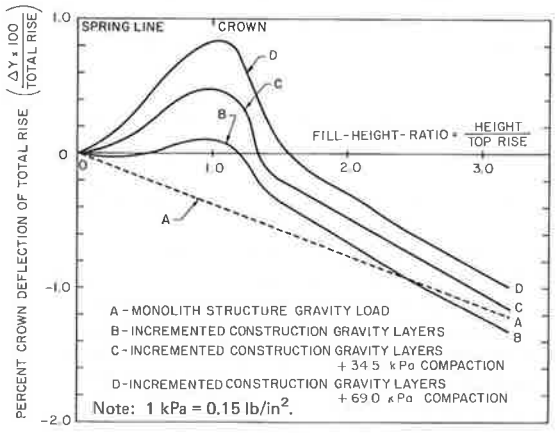

with gravity turned off. Once all the soil is in place, gravity is turned on and the system deforms under its own weight.

A more realistic modeling technique is incremental construction, which attempts to simulate the actual construction process. Here the soil system is divided into a series of soil lifts. Each lift is added into the system one at a time and the structural responses are accumulated.

Figure 4 illustrates the assignment of construction increments used in this study. The reference configuration (unloaded system) includes the liner, footing, in situ soil, and fill soil up to the springline, followed by seven gravity-loaded construction increments from the springline to the top. The reference configuration begins at the springline rather than at the footing level because construction increments placed between the footings and springline tend to hang from the liner in tension and give unrealistic results. [Special nonlinear soil models or interface elements may be used to correct this problem (12).]

The effect of monolith and incremental loading on crown displacement is shown in Figure 6 by curves A and B, respectively. Crown displacement is given as percentage of total rise (positive implies peaking), and is plotted as a function of fill-height ratio. Fill-height ratio is defined as fill height above springline divided by the top rise. Thus, if the fill-height ratio is 1, the current soil height is level with the crown.

Although the monolith structure (curve A) is not a function of intermediate fill heights, it is plotted as a straight line and the assumption is made that fill height corresponds to percentage of gravity so that full fill height implies full gravity.

The obvious difference between curves A and B is that the incremental solution shows a slight peaking when the fill height is near the crown, whereas the monolith solution is incapable of producing such a response. However, as the fill-height ratio increases beyond 2.0, the discrepancy becomes less pronounced. At full height, the crown displacement ratio is 0.92 (monolith/incremental). Other key response ratios at full height are thrust = 1.04 and moment = 1.08. Ratios are monolith divided by incremental evaluated at springline.

Effect of Compaction Loads

Compaction loads are all temporary loads that advertently or inadvertently compact the soil on the sides of the liner (e.g., vehicles, sheepsfoot rollers, heavy equipment, and hand compacters). Field observations indicate that compaction loads contribute more significantly to lateral movement and peaking than does the gravity weight of the soil layer.

A rigorous analytical model of compaction is very

Table 2. Key response ratios at full fill height.

Key Response Ratio	Parameter and Run Number											
	Compaction Loads		Soil Stiffness			Liner Thickness		Liner Shape		Special Features		
	A None	D Double	E One-Half	F Double	G Nonlinear	H Gage 10	I Gage 1	J Low Profile	K Ellipse	L Thrust Beam	M Soil Bin	N Stiff Ribs
Displacement ratio (crown)	1.15	0.85	1.99	0.52	0.88	1.02	0.99	0.83	2.17	0.99	1.09	0.85
Thrust ratio* (near springline)	1.02	0.98	1.01	0.98	0.99	0.99	1.00	0.95	0.90	1.02	1.01	1.01
Moment ratio (near springline)	1.02	0.98	1.69	0.58	0.89	0.69	1.23	1.09	0.71	1.06	1.00	12.1

Notes: For reference, values of run No. C are relative crown displacement = -7.62 cm (-3.002 in), maximum thrust = -15 516.8 kPa/cm (-5522 lb/in), and maximum moment = -17 257.1 N-m/m (-3878 in · lb/in).

*Both maximum moment and maximum thrust generally occured at first node above springline.

Figure 7. Effect of soil stiffness on crown deflection.

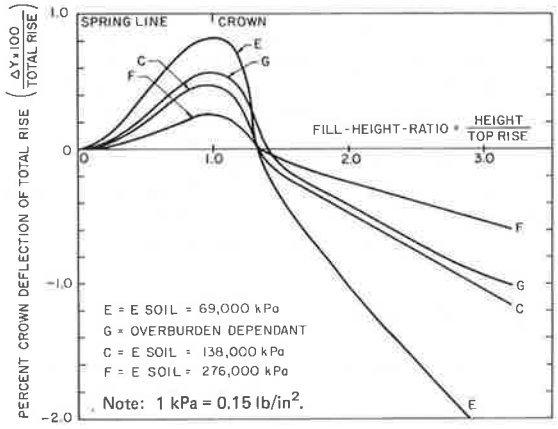

difficult because it requires describing the location, magnitude, and character of all temporary loads, including inertia effects. Moreover, a nonconservative soil model (e.g., plasticity model) must be used so that residual lateral stresses will remain after the compaction load is removed.

In this study a simplified compaction technique is used that simulates the effect of compaction and is applicable for both linear and nonlinear soil models. To start, a uniform pressure, which represents all compaction loads at this level, is applied along the surface of the first construction increment (except for the elements adjacent to the liner) and a solution obtained. Next, the second soil lift is added to the system and another uniform pressure applied to its surface. At the same time, the first pressure load is removed by applying an equal but opposite pressure. These pressures squeeze the second lift and increase lateral pressure on the liner via the Poisson effect. The process is repeated for each lift up to the crown. Above the crown the process is terminated by removing the last compaction pressure so that no compaction loads remain in the system.

The effect of applying this technique is illustrated in Figure 6 by curves B, C, and D (see Table 1), which represent no compaction, 34.5-kPa (5.0-lb/in^2), and 69.0-kPa (10.0-lb/in^2) compaction pressures, respectively. Note that as compaction pressure increases, maximum peaking increases substantially. Indeed, curves C and D are more representative of actual field behavior than curve B (for this reason run C was selected as standard).

As the fill height increases beyond the crown level, the differences between the curves begin to decrease. At full fill height, Table 2 compares ratios between crown displacements by using the basic model (run C) as standard. Each response ratio is formed by dividing the corresponding response of the run number by run C. In addition, comparison ratios are given for maximum moment and thrust located slightly above springline. It is observed that the final effect of compaction loads on maximum moment and thrust is negligible.

Effect of Soil Stiffness

The effect of soil stiffness is examined by specifying Young's modulus of the fill soil as 6900, 13 800, and 27 600 kPa (1000, 2000, and 4000 lb/in^2), corresponding to runs E, C, and F of Table 1. In addition, the effect of a rudimentary nonlinear model known as the overburden-dependent soil model (12) is investigated (run G, Table 1). Here the tangent Young's modulus increases with overburden pressure from a low of 6900 kPa (1000 lb/in^2) to 20 700 kPa (3000 lb/in^2) at full fill-height pressure. In all cases Poisson's ratio is held constant at 0.35 and the in situ soil stiffness is unaltered from the basic model.

Curves E, C, and F in Figure 7 depict the influence of elastic soil stiffness on crown deflection during the construction sequence. Maximum peaking and maximum flattening occur almost in inverse proportion to the soil stiffness. The comparison ratios in Table 2 reveal that thrust is practically unaffected by soil stiffness, whereas moment is influenced in the same manner as displacements but to a lesser degree.

The overburden-dependent model, curve G in Figure 7, shows greater peaking but less flattening than the basic model, curve C. This is expected since the stiffness changes from less than to greater than the basic model as fill height is increased. In summary, it is significant to note that deflection is directly controlled by soil stiffness, whereas thrust is not appreciably changed.

Effect of Liner Gage

The practical range of liner thicknesses for 15 × 5-cm (6 × 2-in) corrugation is gage 10 through 1. In this study, gage sizes 10, 5, and 1 are compared (i.e., runs C, H, and I of Table 1).

Section properties are shown in the insert of Figure 8, and curves C, H, and I show the history of crown deflection for each gage. Interestingly, deflection histories are practically unaffected by the gage even though

Figure 8. Effect of liner gage on crown deflection.

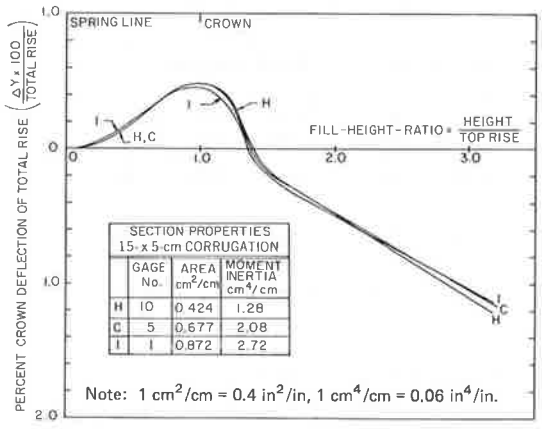

Figure 9. Effect of liner shape on crown deflection.

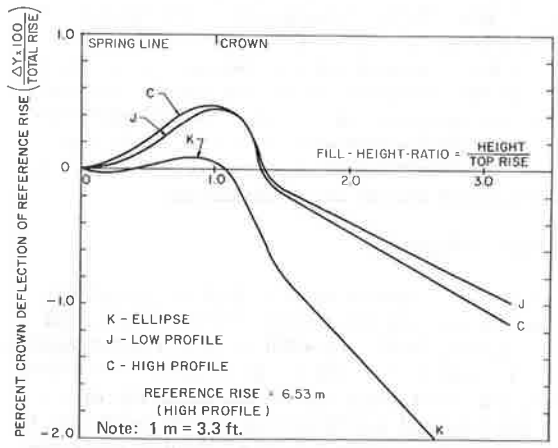

Figure 10. Effect of special features on crown deflection.

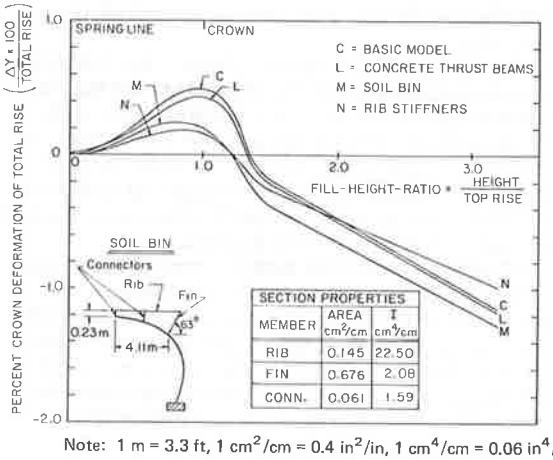

Note: 1 m = 3.3 ft, 1 cm²/cm = 0.4 in²/in, 1 cm⁴/cm = 0.06 in⁴/in.

bending stiffness (moment of inertia) is more than doubled. From the previous study one concludes that soil stiffness dominates liner stiffness and controls the deformed shape. Of course, in the early stages of construction, when the soil height is below the springline, this conclusion is not valid because the soil mass is too small to dominate the system. Here stiff liners are useful to maintain shape and provide lateral resistance for compaction. From Table 2, observe that thrust is unaffected by liner stiffness, whereas moment increases significantly with liner stiffness.

Effect of Liner Shape

Three fundamental shapes are compared: high-profile arch, low-profile arch, and ellipse, corresponding to runs C, J, and K in Table 1. All shapes have the same span and top rise so that the basic finite element mesh (Figure 4) is unaltered above the springline.

To model the ellipse, the bottom half of the basic mesh is replaced by a mirror image of the top half; thus, a horizontal ellipse is formed that has a total rise of 6.81 m (22.3 ft). For the low-profile arch, additional elements are added to raise the floor and footing of the basic mesh to 0.36 m (1.17 ft) below the springline so that the total rise is 3.76 m (12.3 ft). One liner element is used between the springline and the footing and the last element is anchored in the footing to provide continuity.

Figure 9 illustrates the history of crown deflection for each shape as a percentage of the common reference rise, 6.53 m (21.4 ft). Thus, the deflection histories may be compared directly. Note deflections of the high- and low-profile arches follow similar trends, but the high-profile arch is slightly more flexible. However, the ellipse exhibits very little peaking but excessive flattening, more than twice that of the high-profile arch.

Observe in Table 2 that the ellipse affords a moderate reduction of thrust and moment compared to the high-profile arch, whereas the low-profile arch exhibits a slight decrease in thrust and an increase in moment.

Effect of Special Features

The performance of special features (thrust beam, soil bin, and rib stiffeners) illustrated in Figure 2 are compared to each other and the basic model, corresponding to runs C, L, M, and N in Table 1. Note, however, that the finite element idealizations do not mimic all of the intended functions of each special feature. This must be kept in mind when interpreting the results.

To model the thrust beam, triangular continuum elements are added to the basic mesh forming a triangular concrete ear measuring 1.04 m (3.42 ft) on the horizontal leg and 0.71 m (2.33 ft) on the vertical leg. The acute angle is located 3.66 m (12.0 ft) off the center line. Material properties are the same as the concrete footing shown in Figure 3. The ear is assumed part of the initial configuration.

Modeling of the soil bin is approximated by superimposing a steel frame structure on the liner, as shown in the insert of Figure 10. The section properties of the rib and connection members represent smeared averages over the rib spacing interval, whereas the fin is continuous and has the same properties as the liner. Shaped rib stiffeners are easily incorporated into the basic mesh by increasing the sectional properties of the liner. Again section properties are approximated by a smeared average over the rib spacing interval. For this example, the composite liner moment of inertia is 82.0 cm⁴/cm (5.0 in⁴/in) and the composite liner area is 1.12 cm²/cm (0.44 in²/in). Properties approximate a curved I-beam (12WF36) spaced at 1.5-m (5-ft) intervals and bonded to the liner. Note that the stiffened liner is nearly 40 times stiffer in bending than the unstiffened liner.

Curves C, L, M, N in Figure 9 illustrate the effect of each special feature on the history of crown deflection. As might be expected, the rib stiffeners and soil bin substantially limit peaking (curves M and N). How-

ever, as fill height is increased, the soil bin structure exhibits slightly more flattening than the other structures. The thrust beam (curve L) provides a modest reduction in peaking but for the most part behaves like the basic model (curve C). At least one attribute of the thrust beam not modeled in this analysis is that higher compaction (soil stiffness) can be achieved in the soil adjacent to the thrust beam.

At full fill height, Table 2 shows that the maximum moment of the rib-stiffened structure is increased an order of magnitude due to the large increase in bending stiffness. However, other key responses are not significantly altered by the special features.

SUMMARY AND CONCLUSIONS

This study illustrates the influence of fundamental modeling assumptions in applying the finite element method to long-span systems. Based on these studies, the following findings, conclusions, and recommendations are offered:

1. Solutions that use large deformation theory do not differ appreciably from those that use small deformation theory; the discrepancy is less than 8 percent. This discrepancy is due to large rotations, not large strains. Therefore, small deformation theory and infinitesimal stress-strain laws may be used for analyzing long-span systems if the percentage of crown deflection remains within practical limits, say 2 percent.
2. At full fill height a monolith representation yields a solution in approximate agreement (10 percent discrepancy) with an incremented system. However, a monolith system is incapable of tracking the history of deformation such as maximum peaking, nor can it consider compaction loads. As a general rule monoliths have limited value in long-span analysis. Incremented techniques should be used.
3. Compaction pressure placed on each soil-layer increment produces peaking several times greater than the gravity weight of the soil. (This correlates with field observations.) Thus compaction loads should be included in long-span analysis.
4. Soil stiffness (Young's modulus) dictates the magnitude of the liner deformation (i.e., deformation is in inverse proportion to soil stiffness). Since liner deformation is primarily due to bending (as opposed to membrane contraction), the liner bending moments are also inversely proportional to soil stiffness. However, thrust is insensitive to soil stiffness. Evidently, the selection of a soil model (linear or nonlinear) is crucial for predicting the deformed shape of the liner.
5. Liner bending stiffness within the range of standard gage sizes for structural corrugation has negligible effect on controlling liner deformation when the fill soil is above the springline. In other words, the soil stiffness dominates the system so that the deformed shape is not changed when using a heavier gage. As a consequence, the maximum moment increases in proportion to the bending stiffness because the deformed shape does not change appreciably with gage. Thrust remains insensitive to liner gage, therefore thrust stress is reduced in proportion to the sectional area. Rather than conclude that increasing bending stiffness by heavier gage is of no value to reduce deflection, it is recognized that stiff liners are beneficial in early stages of construction to maintain shape and provide compaction resistance.
6. With regard to liner shape, high- and low-profile arches exhibit similar structural responses, but the high profile is slightly more flexible. In contrast, the ellipse exhibits very little peaking but shows excessive flattening due to the simultaneous deformation of top and bottom arches. Correspondingly, thrust is reduced by 10 percent due to increased soil arching.
7. Special features, thrust beam, soil bin, and rib stiffeners exhibit no marked difference in crown deflection at full fill height. However, during the incremental construction process, the circumferentially stiffened structures (soil bin and rib stiffeners) exhibit significantly less peaking than the less-stiffened structures.

The questions pursued in this study are fundamental. It is hoped the findings will provide a foundation or benchmark for other studies. Many more detailed areas of study and experimental programs need to be undertaken before a universally accepted long-span model is established. The area of singular concern is characterization of the soil because it controls the deformation of the entire system. When investigators come to agreement on a soil model, then agreement on an accepted modeling practice of long-span systems is not far behind.

ACKNOWLEDGMENTS

I wish to express appreciation to the Federal Highway Administration and the technical monitor, George P. Ring, for sponsoring this effort. This work is part of an ongoing research study in the Department of Civil Engineering, University of Notre Dame. Thanks are extended to Rene Orillac, research assistant at Notre Dame, for his support in this study.

REFERENCES

1. E. T. Selig, J. F. Abel, F. H. Kulhawy, and W. E. Falby. Review of the Design and Construction of Long-Span, Corrugated-Metal, Buried Conduits. Federal Highway Administration, Technical Rept. HRS-14, Oct. 1977.
2. M. G. Katona and J. M. Smith. A Modern Approach for Structural Design of Pipe Culverts. 2nd International Conference on Computers in Engineering and Building Design. IPC Science and Technology Press Limited, Guildford, Surrey, England, CAD76, 1976.
3. R. J. Krizek and others. Structural Analysis and Design of Pipe Culverts. NCHRP, Rept. 116, 1971.
4. C. B. Brown, D. R. Green, and S. Pawsey. Flexible Culverts Under High Fills. Proc., ASCE, Vol. 94, No. ST4, April 1968.
5. J. F. Abel and R. Mark. Soil Stresses Around Flexible Elliptical Pipes. Proc., ASCE, Vol. 99, No. SM7, July 1973, pp. 509-526.
6. J. M. Duncan. Finite Element Analysis of Buried Flexible Metal Culvert Structures. Laurits Bjerrum Memorial Vol., March 1975.
7. G. A. Leonards. Performance of Pipe Culverts Buried in Soil. Department of Civil Engineering, Purdue Univ., Lafayette, IN.
8. J. F. Abel, G. A. Nasir, and R. Mark. Stresses and Deflections in Soil-Structure Systems Formed by Long-Span Elliptic Pipe. Armco Steel Corp., Princeton Univ., July 1977.
9. J. M. Duncan. Design Studies for a 35-ft. Span Aluminum Culvert for Greenbrier County, West Virginia. Kaiser Aluminum, San Francisco, July 8, 1975.
10. J. M. Duncan. Behavior and Design of Long-Span Metal Culvert Structures. Journal of the Geo-

technical Engineering Division, Proc., ASCE, in press.
11. O. C. Zienkiewicz. The Finite Element Method in Engineering Science. McGraw-Hill Book Co., London, 1971.
12. M. G. Katona and others. CANDE: Engineering Manual—A Modern Approach for the Structural Design and Analysis of Buried Culverts. CANDE: System Manual. CANDE: User Manual. Repts. to the Federal Highway Administration, HRS-14, 1976.
13. K. J. Bathe. ADINA: A Finite Element Program for Automatic Dynamic Incremental Nonlinear Analysis. Acoustics and Vibration Laboratory, Department of Mechanical Engineering, MIT, Cambridge, Rept. 82448-1, 1975.

Publication of this paper sponsored by Committee on Subsurface Soil-Structure Interaction.